# Structural and theoretical analysis of some mesogenic azines containing strong electron donor–acceptor groups

**Roberto Centore and Carmine Garzillo**

*Dipartimento di Chimica, Università di Napoli 'Federico II', Via Mezzocannone 4, 80134 Napoli, Italy*

**A structural and theoretical analysis of some mesogenic bis(phenylene)azines containing a methyl group on the azine system and strong electron donor–acceptor groups on the phenylene rings is reported. Starting from the X-ray molecular structures and with the support of semiempirical quantum mechanical calculations, the structural and conformational properties of the azines are analysed and compared with recent literature data on similar acetophenone azines. Some geometrical and electronic data of the molecules are also calculated and discussed in the paper, which may be useful for a better understanding of the mesophasic behaviour of the compounds.**

## Introduction

In an earlier paper we reported the crystal structure analysis of some mesogenic aromatic azines containing electron donor–acceptor groups, of potential interest in the non-linear optics (NLO) field.[1]

A conformational variability, mainly due to torsion around the central N–N bond, but also around C–C bonds connecting the azine system to phenyl rings, was found. This variability had already been found by us[2,3] and others[4-6] in acetophenone azines, some of which also contained donor–acceptor groups[7] and may be considered a consequence of the low torsional barrier around the N–N bond.[5-6]

Several liquid crystal molecules possess in the so-called mesogenic groups, chemical bonds having relatively low energy torsions. For example, the well-known mesogenic cores *p*,*p*′-biphenylene, *p*-oxybenzoate and *p*-phenylene-terephthalate esters.

These conformational degrees of freedom are gained on melting; therefore, the actual average shape of the molecules in the liquid crystal phase may change from that of the crystal phase particularly if the direction of the conformationally variable chemical bonds is not collinear with the long molecular axis. This, in turn, may affect the liquid crystal behaviour, as it depends on the geometrical features of the molecule (*e.g.* the axial ratio).[8,9]

Theoretical analysis of the fundamental electronic state of mesogenic molecules may be useful for an estimate of the torsional barriers and, therefore, for a more precise definition of the rigidity and of the actual molecular geometry (and possibly dynamics) in the liquid crystal phase.

The analysis of the electronic excited states of mesogenic molecules may also have some interest for the study of liquid crystal behaviour. In fact, the orientation-dependent part of the dispersive intermolecular forces, which also contribute to the stabilization of the liquid crystal phase, particularly of the long range orientational order of nematics, depends on the spatial anisotropy of molecular transition moments from fundamental to excited electronic states (molecular anisotropy factor[10]).

In the framework of current molecular theories of liquid crystals, the axial ratio and the molecular anisotropy factor (or related quantities such as molecular polarization anisotropy) are the only strictly molecular parameters which are considered explicitly.[8,9,11]

In the present paper a theoretical analysis of the following four azines **2**–**5** is reported.

The close chemical and structural similarity of these azines

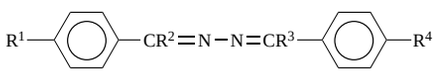

| | | | | |
|---|---|---|---|---|
| **2** | $R^1 = CH_3O$ | $R^2 = CH_3$ | $R^3 = H$ | $R^4 = CN$ |
| **3** | $R^1 = CH_3O$ | $R^2 = H$ | $R^3 = CH_3$ | $R^4 = CN$ |
| **4** | $R^1 = (CH_3)_2N$ | $R^2 = H$ | $R^3 = CH_3$ | $R^4 = CN$ |
| **5** | $R^1 = (CH_3)_2N$ | $R^2 = H$ | $R^3 = CH_3$ | $R^4 = NO_2$ |

should allow a significant, comparative analysis of their structure–property relationships. The acetophenone azines have been investigated in detail by Glaser and co-workers both experimentally and theoretically;[5-7] the present compounds, however, have a less substituted azine system (only one methyl group is present), which offers the possibility of extending the analysis of the conformational properties of the azine system in locally less symmetrical and less sterically hindered environments.

Azines **2** and **3** are nematogenic[1] (isotropization temperatures 450.1 and 439.2 K, respectively), for **4** a monotropic nematic phase is observed, while **5** is not mesogenic. The synthesis and crystal structures of **2** and **3** have already been described by us.[1] The synthesis and crystal structure of **4**, 4-dimethylaminobenzaldehyde (4-cyanopheny/ethylidene)hydrazone (*E*,*E*), and **5**, 4-dimethylaminobenzaldehyde (4-nitrophenylethylidene)hydrazone (*E*,*E*), are also reported in the present paper.

## Experimental

Compounds **4** and **5** were prepared by reaction of commercial *N*,*N*-dimethylaminobenzaldehyde with *p*-cyanoacetophenone hydrazone and *p*-nitroacetophenone hydrazone, respectively. Reaction conditions were similar to those described previously by us for **2** and **3**.[1] The synthesis of hydrazones has also been reported.[12] Azines **4** and **5** were purified by repeated crystallisations from ethanol; single crystals suitable for X-ray diffraction analysis were obtained by evaporation from saturated ethanolic solutions, as yellow plates for **4** and orange plates for **5**.

Weissenberg and oscillation photographs suggested orthorhombic symmetry and the *Pbca* space group for both **4** and **5**. Preliminary cell constant calculations and diffraction pattern inspection suggested the two compounds be truly isomorphous in the crystal phase. This was later confirmed by the structural analysis.

Accurate cell parameters for both compounds were obtained through a least-squares fit to the setting angles of 25, accurately

**Table 1** Crystal, collection and refinement data for **4** and **5**[a]

| | **4** | **5** |
|---|---|---|
| Chemical formula | $C_{18}H_{18}N_4$ | $C_{17}H_{18}N_4O_2$ |
| Crystal system | Orthorhombic | Orthorhombic |
| Space group | *Pbca* | *Pbca* |
| *a*(/Å) | 37.395(4) | 37.654(5) |
| *b*(/Å) | 11.371(2) | 11.343(4) |
| *c*(/Å) | 7.5383(8) | 7.447(5) |
| *V*(/Å$^3$) | 3205.5(7) | 3181(2) |
| *Z* | 8 | 8 |
| $d_c$/Mg m$^{-3}$ | 1.203 | 1.296 |
| $\mu$/cm$^{-1}$ | 5.466 | 6.772 |
| *T*/K | 295 | 295 |
| Crystal size mm$^3$ | 0.3 × 0.2 × 0.1 | 0.5 × 0.5 × 0.03 |
| Reflections collected | 3297 | 3269 |
| Range of indices | $0 < h < 46$, $-14 < k < 0$, $0 < l < 9$ | $0 < h < 47$, $0 < k < 14$, $-9 < l < 0$ |
| Reflection observed $[I > 3\sigma(I)]$ | 2274 | 1522 |
| $\theta$ max | 74.9° | 74.9° |
| Parameters refined | 271 | 262 |
| *R* | 0.048 | 0.064 |
| *wR*, *S* | 0.067, 1.984 | 0.090, 1.633 |
| Max. and min. peaks in the final difference Fourier map (e Å$^{-3}$) | +0.191, −0.188 | +0.366, −0.240 |
| Weights | $\frac{4F_o^2}{[\sigma^2(F_o^2) + (0.04F_o^2)^2]}$ | $\frac{4F_o^2}{[\sigma^2(F_o^2) + (0.08F_o^2)^2]}$ |
| Max. shift to error ratio in the last refinement cycle | 0.01 | 0.01 |

[a] Atomic coordinates, bond lengths and angles, and thermal parameters have been deposited at the Cambridge Crystallographic Data Centre (CCDC). For details of the deposition scheme, see 'Instructions for Authors', *J. Chem. Soc., Perkin Trans. 2*, 1997, Issue 1. Any request to the CCDC for this material should quote the full literature citation and the reference number 188/36.

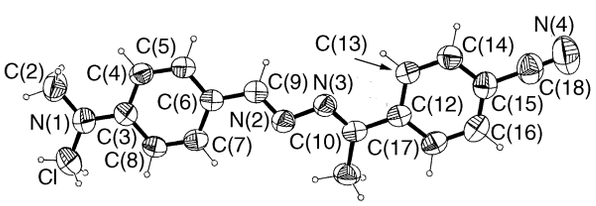


**Fig. 1** X-Ray structure of the azine **4**

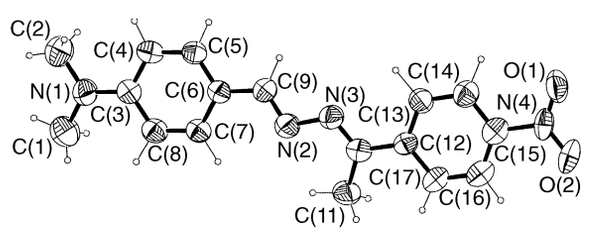


**Fig. 2** X-Ray structure of the azine **5**

centred, strong reflections, in the range $15° < 2\theta < 25°$, on an Enraf-Nonius CAD-4 automated single crystal diffractometer, using graphite monochromated Cu-Kα radiation. Data collection was performed in the range $1° < \theta < 75°$, in the $\omega/\theta$ scan mode for both compounds. During data collection the intensity of a control reflection, periodically measured, showed only random fluctuations. Lorentz and polarization corrections were applied, no correction for absorption and secondary extinction was introduced. Details of data collection and refinement are reported in Table 1.

The structure of **4** (Fig. 1) was solved by direct methods. The rantan option of the MULTAN 82 program[13] gave all non-H atoms of the crystallographically independent molecule. For azine **5** (Fig. 2), on the basis of the assumed isomorphism with **4**, refined atomic coordinates of all atoms of **4**, except those of the terminal cyano group, were taken as the starting model. After scale factor refinement and structure factor calculation, a difference Fourier map readily gave the three atoms of the missing nitro group, as the first three maxima.

For both compounds, refinement was performed by the full-matrix least-squares method with anisotropic thermal parameters for C, O, N atoms, using the SDP package[14] running on a MicroVAXII computer. Coordinates and individual isotropic thermal parameters of H atoms (whose positions were initially determined in a difference Fourier map) were refined for **4**, while only coordinates of H atoms were refined for **5**, thermal parameters being fixed equal to those of the carrier atom. ORTEP[15] and PLUTO[16] programs were used for molecular and crystal drawings.

Differential scanning calorimetric analysis was performed under a nitrogen atmosphere, at a heating–cooling rate of 10 K min$^{-1}$, using a Perkin-Elmer DSC7 apparatus. Optical observations were made on a Leitz Axioskop polarizing microscope equipped with a Mettler FP5 hot stage. UV–VIS absorption spectra were recorded in acetonitrile solutions, at ambient temperature, on a Perkin-Elmer Lambda 7 UV–VIS spectrophotometer.

Molecular structures and N–N rotational profiles were obtained by MNDO/CI semiempirical scheme (PM3 parametrization,[17] MOPAC93 package[18]). X-Ray molecular structures were fully optimized and rotational profiles reported in Fig. 3 were calculated with 'frozen geometry' paths, allowing us to vary the torsion angle alone around the central N–N bond. Because of high density of electronic levels falling at energies lower than those of the three highest occupied molecular orbitals (MOs) and higher than those of the three lowest unoccupied MOs, the size of the active space to be used in the computation can be kept within reasonable limits if the computation includes just the singly excited configurations or, alternatively, if just configurations generated by the MOs mentioned above are considered. We have made the latter choice, since computations at the INDO/S level have shown that the above MOs have predominant weights in the wave-function of the lower excited singlets. Molecular polarizability tensors were

**Table 2** Bond lengths (Å), selected bond angles (°) and torsion angles (°), with estimated standard deviations in parentheses, for **4** and **5**

| | **4** | **5** | | **4** | **5** |
|---|---|---|---|---|---|
| C1–N1 | 1.449(3) | 1.443(5) | C1–N1–C2 | 118.6(2) | 118.3(4) |
| C2–N1 | 1.443(2) | 1.454(6) | C1–N1–C3 | 120.5(2) | 121.6(3) |
| N1–C3 | 1.367(2) | 1.366(4) | C2–N1–C3 | 120.9(2) | 119.9(3) |
| C3–C4 | 1.404(2) | 1.401(5) | C6–C9–N2 | 122.3(1) | 121.3(3) |
| C3–C8 | 1.415(2) | 1.417(5) | C9–N2–N3 | 111.8(1) | 112.3(3) |
| C4–C5 | 1.377(2) | 1.387(5) | N2–N3–C10 | 114.8(1) | 114.2(3) |
| C5–C6 | 1.394(2) | 1.391(4) | N3–C10–C11 | 124.8(1) | 124.3(3) |
| C6–C7 | 1.397(2) | 1.394(5) | N3–C10–C12 | 115.7(1) | 116.2(3) |
| C7–C8 | 1.369(2) | 1.387(5) | C11–C10–C12 | 119.5(2) | 119.5(3) |
| C6–C9 | 1.448(2) | 1.449(4) | C15–C18–N4 | 179.5(2) | |
| C9–N2 | 1.277(2) | 1.274(4) | C15–N4–O1 | | 118.6(3) |
| N2–N3 | 1.405(2) | 1.405(4) | C15–N4–O2 | | 118.0(4) |
| C10–N3 | 1.284(2) | 1.295(4) | O1–N4–O2 | | 123.4(4) |
| C10–C11 | 1.502(2) | 1.508(5) | | | |
| C10–C12 | 1.479(2) | 1.479(5) | | | |
| C12–C13 | 1.399(2) | 1.398(5) | | | |
| C12–C17 | 1.398(2) | 1.391(4) | | | |
| C13–C14 | 1.378(2) | 1.392(5) | C1–N1–C3–C4 | 178.2(2) | 174.9(4) |
| C14–C15 | 1.385(2) | 1.389(5) | C2–N1–C3–C8 | 178.3(2) | −179.9(4) |
| C15–C16 | 1.386(2) | 1.372(5) | C5–C6–C9–N2 | 173.9(2) | 171.8(4) |
| C16–C17 | 1.379(2) | 1.385(5) | C9–N2–N3–C10 | −162.9(2) | −161.7(4) |
| C15–C18 | 1.443(2) | | N3–C10–C12–C17 | 170.6(2) | 170.1(4) |
| C18–N4 | 1.139(2) | | O1–N4–C15–C14 | | 2.7(6) |
| C15–N4 | | 1.469(5) | O2–N4–C15–C16 | | 2.1(7) |
| N4–O1 | | 1.204(5) | | | |
| N4–O2 | | 1.211(4) | | | |

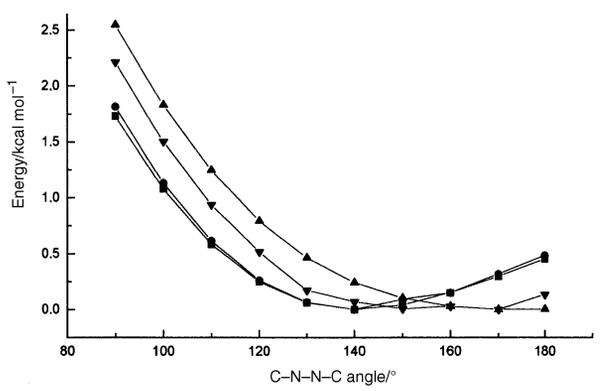


**Fig. 3** Rotational profiles: ■ **2**; ● **3**; ▲ **4**; ▼ **5**

obtained with time dependent Hartree–Fock calculations at 0.0 eV field (POLAR keyword [18,19]); they were computed at the absolute minimum of the molecular energy and at torsion angles around the central N–N bond of 110° and 180° with frozen geometry paths.

## Results and discussion

Azines **4** and **5** show solid state polymorphism, which is briefly discussed.

For **4**, in particular, evidence of several different crystal phases has been found. A sketch of the phase transformations of azine **4** is shown in Scheme 1 (temperature in K).

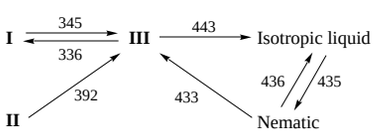


**Scheme 1** Phase behaviour of **4**

The as-prepared, solution-crystallized, sample contains at least two different crystal modifications, which also have different crystal morphologies: elongated prisms (phase I) and large plates (phase II). The crystal phase whose structure is described below (phase II) transforms irreversibly, at 392 K, into a new crystal phase, phase III. On cooling phase III, phase II is no longer obtained, but, at 336 K, phase I is obtained. Phase III may also be obtained by heating crystals of phase I above 345 K. The transition I ⟶ III is a reversible one ($\Delta H$ = 0.39 kcal mol$^{-1}$) (1 cal = 4.184 J) and, furthermore, is topotactic (*i.e.* single crystals are not broken through the transition). By heating phase III, melting to isotropic liquid takes place at 443 K. On cooling the isotropic liquid phase of **4**, in a narrow temperature range before crystallization occurs, an anisotropic liquid phase may be observed under the polarizing microscope, whose mobile schlieren morphology suggests a nematic nature. If the nematic phase is rapidly heated, isotropization occurs at 436 K, which is below the melting temperature of phase III. The liquid crystal phase, therefore, is a monotropic one, being metastable with respect to phase III. It is interesting to note, however, that the isotropization temperature of **4** is very close to that of the similar compound **3**.[1]

As far as azine **5** is concerned, the crystal phase described in this paper transforms irreversibly at 423 K into a second crystal phase, which melts at 478 K, and is restored again on cooling the isotropic liquid phase.

Refined bond lengths, bond angles and selected torsion angles are reported in Table 2 for **4** and **5**; molecular drawings are reported in Figs. 1 and 2.

Bond lengths and angles of **4** and **5** are consistent within experimental error. The conformations of the two molecules are almost identical. In crystals of **4** and **5**, molecules adopt a substantially planar conformation, the dihedral angles between average planes of the phenyl ring being 3.3(8)° and 3(2)° for **4** and **5**, respectively. This is the result of a close s-*trans* conformation around the N–N bond [torsion angles −162.9(2)° for **4** and −161.7(4)° for **5**] and of *trans* planar conformations around C6–C9 and C10–C12 bonds; in particular, in **4** and **5**, phenyl twist with respect to C=N–N plane is almost absent and equal on both sides of the azine system, *i.e.* the methyl group has no particular effect on the phenyl twist.

A planar trigonal geometry is observed around the N atom of the amino group. The sp$^2$ hybridization of this atom should favour electron donation to the adjacent phenyl ring. This is consistent with the observed shortened length of the N1–C3 bond [20] and also with the observation that C4–C5 and C7–C8 bond lengths in the phenyl ring adjacent to the dimethylamino

**Table 3** UV–VIS absorption data of azines

| Azine | $\lambda_{max}(CH_3CN)$/nm; $\varepsilon_{max}$/dm$^3$ mol$^{-1}$ cm$^{-1}$ | | | |
|---|---|---|---|---|
| **2** | | 264; $1.1 \times 10^4$ | 323; $2.6 \times 10^4$ | |
| **3** | 213; $1.6 \times 10^4$ | 262; $1.1 \times 10^4$ | 322; $3.3 \times 10^4$ | |
| **4** | | 264; $1.0 \times 10^4$ | 384; $2.3 \times 10^4$ | |
| **5**[a] | 222 | 306 | 349 | 402 |

[a] $\varepsilon_{max}$ not evaluated because of the low solubility of the compound.

**Table 4** Selected bond lengths (Å), bond angles (°) and torsion angles (°) for the optimized geometry of azines

| | | | |
|---|---|---|---|
| Azine **2**[a] | | | |
| C5–C8 | 1.476 | C6–C5–C8–N1 | −166.94 |
| C8–N1 | 1.310 | C8–N1–N2–C10 | −141.29 |
| N1–N2 | 1.377 | N2–C10–C11–C12 | 14.19 |
| C10–N2 | 1.300 | | |
| C10–C11 | 1.468 | | |
| Azine **3**[a] | | | |
| C5–C8 | 1.464 | C6–C5–C8–N1 | −173.18 |
| C8–N1 | 1.302 | C8–N1–N2–C10 | −140.97 |
| N1–N2 | 1.377 | N2–C10–C11–C16 | 14.00 |
| C10–N2 | 1.308 | | |
| C10–C11 | 1.480 | | |
| Azine **4** | | | |
| N1–C3 | 1.441 | C1–N1–C2 | 111.75 |
| C6–C9 | 1.463 | C1–N1–C3 | 116.71 |
| C9–N2 | 1.303 | C2–N1–C3 | 116.71 |
| N2–N3 | 1.387 | C1–N1–C3–C4 | 160.33 |
| C10–N3 | 1.306 | C2–N1–C3–C8 | −160.87 |
| C10–C12 | 1.481 | C5–C6–C9–N2 | −176.80 |
| C18–N4 | 1.160 | C9–N2–N3–C10 | −172.22 |
| | | N3–C10–C12–C17 | 144.64 |
| Azine **5** | | | |
| N1–C3 | 1.441 | C1–N1–C2 | 111.78 |
| C6–C9 | 1.463 | C1–N1–C3 | 116.80 |
| C9–N2 | 1.303 | C2–N1–C3 | 116.71 |
| N2–N3 | 1.381 | C1–N1–C3–C4 | 160.87 |
| C10–N3 | 1.306 | C2–N1–C3–C8 | −160.59 |
| C10–C12 | 1.481 | C5–C6–C9–N2 | 175.55 |
| O1–N4 | 1.215 | C9–N2–N3–C10 | −152.44 |
| O2–N4 | 1.215 | N3–C10–C12–C17 | 148.01 |

[a] Atomic numbering as in ref. 1.

group are systematically shorter than the remaining four in both **4** and **5**. Similar distortions of phenyl ring geometry towards a quinoid structure have already been observed in *N*,*N*-dialkylanilines containing strong electron-acceptor groups (*e.g.* *N*,*N*-diethyl-*p*-nitroaniline,[21] *N*,*N*-dimethyl-*m*-nitroaniline[22]) and are consistent with the electron-withdrawing character of the azine system as a whole;[6] it is also interesting to note that no such distortion of the phenyl ring geometry is observed for the ring C12···C17 to which a strong electron-acceptor group is already attached (cyano and nitro groups). The C6–C9 bond distance in **4** and **5** is significantly shorter than the corresponding distance in azines **1** and **3** of ref. 1: 1.448(2) and 1.449(4) Å for **4** and **5** as compared with 1.456(2) Å for A and B molecules of **3** and 1.464(3) Å for **1**. This should also be a consequence of the strong electron-donor effect of the dimethylamino group as compared with the methoxy group, coupled with the electron-withdrawing character of the azine system as a whole (push–pull pattern); in this pattern, however, it should be noted that the expected lengthening of the C9=N2 bond distance in **4** and **5**, as compared with **3**, is not observed or is not statistically significant. With the exception of the C6–C9 bond distance, the pattern of the bond lengths and angles in the azine system of **4** and **5** is practically coincident with that of **3** in which, however, a non-planar molecular conformation is observed[1] (dihedral angles between the planes of the phenyl rings are *ca.* 47° and *ca.* 58° for the two crystallographically independent molecules, A and B).

UV–VIS absorption spectra of **2**, **3** and **4** are quite similar, Table 3. A very intense band is present in the range 300–400 nm ($\pi \longrightarrow \pi^*$) with a shoulder at shorter wavelengths (*ca.* 260 nm), which is well resolved for **4** only. The peak position of the most intense band is almost coincident for **2** and **3**, while significant red-shift is observed for **4**. This auxochromic effect of the *N*,*N*-dimethylamino group should correspond to a partial delocalization of the lone pair of N atom onto the π conjugated system of the molecule, which is consistent with solid state and 'gas phase' (see below) structural results.

Selected data for the optimized 'gas phase' geometry of azines **2**, **3**, **4** and **5** are reported in Table 4.

For azines **4** and **5**, in particular, the geometry around the N atom of the dimethylamino group is not strictly planar trigonal, *i.e.* a slight distortion towards a pyramidal geometry is observed; consistent with this, longer N1–C3 and C6–C9 bond lengths are found, as compared with crystal structure values. This behaviour is consistent with microwave spectroscopy data for *N*,*N*-dimethylaniline.[23] Distortions of the phenyl ring bonded to the dimethylamino group towards the 'quinoid' structure are also observed. Phenyl twist around C10–C12 bond is significantly higher than for the C6–C9 bond. Torsion angles around the N2–N3 bond, on the other hand, are within ±10° of the crystal phase value.

The optimized geometry of **3** is very close to that found in the crystal structure, both for the torsion angle around the N–N bond and for the phenyl twist with respect to the C=N–N plane. In this case, also, phenyl twist is more pronounced by the methyl side of the azine system. The calculated conformation of **2** is different from that in the crystal; in particular, the conformation around N–N is not s-*trans*, the torsion angle being close to the value found for **3**. We conclude, therefore, that the planar conformation observed for **2** in the crystal phase is the result of crystal packing effects. The stacked packing of molecular sheets of **2** in the crystals, as described in ref. 1, agrees with this picture.

The calculated internal energy as a function of the torsion angle $\tau$ around the N–N bond is reported in Fig. 3 for azines **2**–**5**. The minimum energy corresponds to a close to s-*trans* conformation for **4** only. However, a common feature of the four azines rests in the very low torsional barrier. The torsional potential is less than 1 kcal mol$^{-1}$ up to $\tau$ values of 120° for **4** and 110° for the others, and, also at $\tau$ *ca.* 90°, the potential is less than 2.6 kcal mol$^{-1}$ for all compounds. We recall, for comparison only, the energy barriers[24] for ethane, which is 2.8 kcal mol$^{-1}$ and for 1,3-butadiene, which is 4.9 kcal mol$^{-1}$. These results, which are consistent with those reported by Glaser and co-workers for some acetophenone azines,[5,25] clearly indicate that changes in the conformation around the N–N bond, at least in the $\tau$ range of *ca.* 180–150°, which is the experimentally observed range of variability of our compounds, may be easily produced by crystal packing, as they are not of high energy.

The crystal packing of **4** is reported in Fig. 4. Molecules of **4** and **5** are packed with their long axes directed approximately along *a*. Laterally adjacent molecules, along *b* and *c*, form layers which are piled up along *a* at distances of *a*/2. Crystal packing may also be described as a succession of molecular rows parallel to *a*, laying on the lattice planes of the family (021), which are spaced at $d_{021}$ = 4.5 Å. Within each lattice plane, adjacent molecular rows are spaced at $2d_{0\bar{4}2} = d_{021}$ = 4.5 Å. These pictures are consistent with 021 and 200 being the strongest reflections of the observed diffraction pattern. Within each layer, face-to-face and face-to-edge contacts between planes of laterally adjacent molecules are observed. For the former, typical graphite-like distances between molecular planes are observed (*ca.* 3.4 Å) while distances slightly longer (*ca.* 3.8 Å) are observed for the face-to-edge interactions. In the *a* direction, molecules are probably held together mainly by dipolar interactions between *N*-methyl and cyano (or nitro) groups.

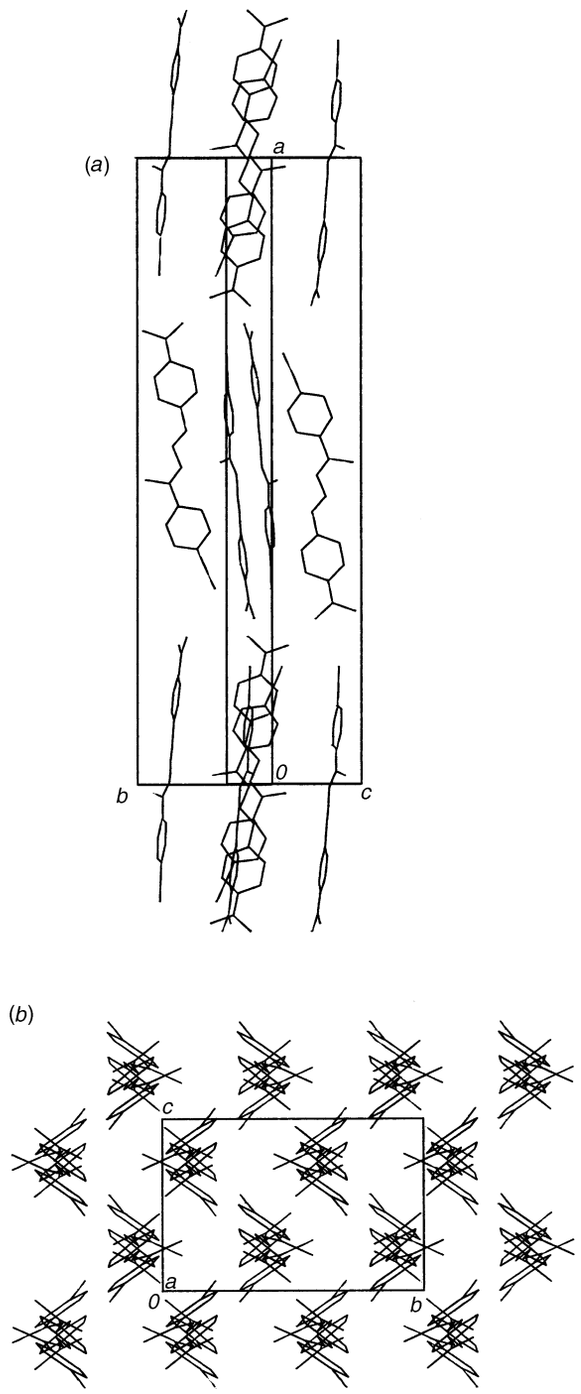


**Fig. 4** The crystal packing of the azine **4**

Principal moments of inertia of the four molecules under investigation are reported in Table 5 for the geometry observed in the crystal phase. They have been evaluated for **4** and **5** as reported previously for **2** and **3**.[1] Other geometric data related to the axis of least inertia have also been calculated and reported in Table 6. The axis of least inertia is practically coincident with the axis of molecular elongation, as it corresponds to a least-squares fitted line through the atoms, taking atomic masses as weights. The pattern of Table 5 clearly indicates that: (*a*) azines **2**, **4** and **5** are almost planar ($I_1 + I_2 \cong I_3$), while **3** is not, which is consistent with the crystallographic results; (*b*) the four molecules all have a highly anisometric shape, the lowest principal moment of inertia being, on average, twenty times smaller than the other two.

The first column of Table 6 shows the average distance from the axis of least inertia for the four molecules; this could be taken as a measure of the average (half) cross section of the

**Table 5** Principal moments of inertia (in units $10^{-46}$ kg m$^2$) for azines **2–5**[a]

| Azine | $I_1$ | $I_2$ | $I_3$ |
|---|---|---|---|
| **2A** | 48.96 | 1057.03 | 1104.28 |
| **2B** | 49.36 | 1053.18 | 1101.06 |
| **2C** | 49.80 | 1052.93 | 1100.95 |
| **2D** | 49.85 | 1057.06 | 1105.43 |
| **3A** | 54.47 | 1041.78 | 1084.55 |
| **3B** | 49.79 | 1056.51 | 1088.93 |
| **4** | 60.61 | 1178.51 | 1236.80 |
| **5** | 66.09 | 1358.19 | 1421.79 |

[a] Data for azines **2** and **3** have been taken from ref. 1.

**Table 6** Geometric data

| Azine | $\langle d \rangle$/Å [a] | $d_{max}$/Å [b] | $L$/Å [c] | $x$ [d] |
|---|---|---|---|---|
| **2A** | 1.22 | 2.87 | 17.1 | 2.97 |
| **3A** | 1.34 | 2.98 | 16.8 | 2.82 |
| **3B** | 1.29 | 2.85 | 17.0 | 2.98 |
| **4** | 1.39 | 2.95 | 17.0 | 2.88 |
| **5** | 1.38 | 2.92 | 16.8 | 2.88 |

[a] Average atomic distance from the axis of least inertia. [b] Maximum atomic distance from the axis of least inertia. [c] Length of the molecules measured along the axis of least inertia. [d] Axial ratio [$x = L/(2d_{max})$].

molecules. The maximum distance from the axis of least inertia (second column of Table 6) is almost constant for the molecules, as it is determined by the methyl group on the azine system. The projection of the head to tail molecular distance onto the axis of least inertia, $L$, is also constant for the molecules, and it should correspond to the length of the major axis of the ellipsoid of revolution of the molecule. An approximate evaluation of the axial ratio, $x$, may be readily obtained by dividing $L$ by the maximum diameter of the molecule (*i.e.* $2d_{max}$); these values are reported in the last column of Table 6: they are close to 3, which is a typical value for common mesogenic molecules.[9] Data in Table 6 indicate only minor geometric differences, if any, among the four molecules (*i.e.* maximum differences in molecular dimensions of Table 6 are not greater than 0.3 Å).

The conformational variability of these molecules, due to the low torsional barrier abound the N–N bond, is fully compatible with displaying liquid crystalline nematic behaviour. The axial ratio of the molecules, evaluated as described above, shows a slight increase when the conformation around the N–N bond changes from *trans* to *gauche*; as an example, for $|\tau|$ in the range 91–93°, $x$ is 3.23, 3.30, 3.10 and 3.07 for **2**, **3B**, **4** and **5**, respectively. It may be inferred, therefore, that an appreciable population of s-*gauche* conformers exists in the nematic phase of these compounds. A similar analysis might be also performed for conformational changes involving phenyl twist around the C6–C9 and C10–C12 bonds, whose directions are almost parallel to the N–N bond (an estimate of the torsional barrier, which is low, is given in ref. 25). The only chemical bonds whose torsions might significantly reduce the axial ratio around are C9–N2 and C10–N3, whose conformation is blocked by the double bond.

From a preliminary analysis of the excited electronic states, we have calculated molecular transition moments for the singly excited states of the four molecules. In particular, it is found that the transition corresponding to the most intense peak in the UV–VIS spectrum of the molecules ($\pi \longrightarrow \pi^*$ transition) has a strong polarization along the long molecular axis.

From the calculated molecular polarizability tensor, we have evaluated mean static polarizability, $\bar{\alpha}$, and polarization anisotropy, $\Delta\alpha$, according to relation (1); ($x$, $y$, $z$) is a

$$\bar{\alpha} = \tfrac{1}{3}(\alpha_{xx} + \alpha_{yy} + \alpha_{zz}),\ \Delta\alpha = \alpha_{xx} - \tfrac{1}{2}(\alpha_{yy} + \alpha_{zz}) \qquad (1)$$

**Table 7** Calculated polarizability data for the azines

| Azine | $\alpha$/Å$^3$ | $\Delta\alpha$/Å$^3$ | $\Delta\alpha/\alpha$ |
|---|---|---|---|
| **2** | 30.09 | 42.01 | 1.40 |
| **3** | 30.13 | 42.17 | 1.40 |
| **4** | 32.57 | 45.33 | 1.39 |
| **5** | 32.04 | 41.53 | 1.30 |

cartesian frame with origin in the molecular centre of mass and axes coincident with the principal axes of inertia of the molecule.

These data are reported in Table 7, together with the ratio $\Delta\alpha/\alpha$ which is directly related to the strength of the anisotropic dispersion energy,[26,27] for the optimized geometry of the molecules.

The most interesting feature of these data rests in the high values of $\Delta\alpha/\alpha$, which are greater than 1 for the four azines.

Calculated $\Delta\alpha/\alpha$ values are little affected by changes of the torsion angle, $\tau$, around the central N–N bond, at least for $\tau$ values corresponding to the flat region of curves of Fig. 3. As an example, for $\tau$ between 110° and 180°, calculated $\Delta\alpha/\alpha$ values are 1.38–1.40 for **2**, 1.38–1.41 for **3**, 1.36–1.39 for **4** and 1.26–1.29 for **5**.

The lack of direct experimental data on polarizability of the studied compounds prevents full confidence being given in the data of Table 7. Also, accurate theoretical calculations of molecular polarizabilities are rather difficult to obtain with more complex methods. For these reasons, we cautiously think that the data in Table 7 have significance mainly at a comparative level; furthermore, it should also be noted that the data in Table 7 refer to 'gas phase' molecules, while a lowering of these values should be expected when the dielectric nature of the material is taken into account.

With this limitation, too, these data and the geometric data discussed above are consistent with the mesophasic behaviour of azines and, in particular, with the close isotropization temperatures of **2**, **3** and **4**.

## Acknowledgements

We are grateful to the Centro Interdipartimentale di Metodologie Chimico Fisiche of the University of Naples 'Federico II' for making Enraf Nonius CAD4 diffractometer available. Many thanks are due to Professor Augusto Sirigu of the University of Naples 'Federico II', for critical reading of the manuscript and helpful suggestions.

## References

1 R. Centore, B. Panunzi and A. Tuzi, *Z. Kristallog.*, 1996, **211**, 31.
2 R. Centore, M. R. Ciajolo, A. Roviello, A. Sirigu and A. Tuzi, *Mol. Cryst. Liq. Cryst.*, 1990, **185**, 99.
3 R. Centore, M. R. Ciajolo and A. Tuzi, *Mol. Cryst. Liq. Cryst.*, 1993, **237**, 185.
4 M. R. Ciajolo, A. Sirigu and A. Tuzi, *Acta Crystallogr., Sect. C*, 1985, **41**, 483.
5 G. S. Chen, M. Anthamatten, C. L. Barnes and R. Glaser, *Angew. Chem., Int. Ed. Engl.*, 1994, **33**, 1081.
6 R. Glaser, G. S. Chen, M. Anthamatten and C. L. Barnes, *J. Chem. Soc., Perkin Trans. 2*, 1995, 1449.
7 G. S. Chen, J. K. Wilbur, C. L. Barnes and R. Glaser, *J. Chem. Soc., Perkin Trans. 2*, 1995, 2311.
8 P. J. Flory, *Adv. Polym. Sci.*, 1984, **59**, 1.
9 G. R. Luckhurst, *Ber. Bunsenges. Phys. Chem.*, 1993, **97**, 1169.
10 W. Maier and A. Saupe, *Z. Naturforsch., Teil A*, 1959, **14**, 882.
11 G. R. Luckhurst, in *Recent Advances in Liquid Crystalline Polymers*, ed. L. L. Chapoy, Elsevier, London and New York, 1985, ch. 7, p. 105 and references therein.
12 R. Centore, B. Panunzi, A. Roviello, A. Sirigu and P. Villano, *Mol. Cryst. Liq. Cryst.*, 1996, **275**, 107.
13 P. Main, S. S. Fiske, S. E. Hull, L. Lessinger, G. Germain, J. P. Declerq and M. M. Woolfson, MULTAN11/82. A system of computer programs for the automatic solution of crystal structures from X-ray diffraction data. Universities of York, England, and Louvain, Belgium, 1982.
14 Enraf-Nonius, Structure determination package, Enraf-Nonius, Delft, The Netherlands, 1985.
15 C. K. Johnson, ORTEPII. Report ORNL-5138. Oak Ridge National Laboratory, Tennessee, USA, 1976.
16 W. D. S. Motherwell and W. Clegg, PLUTO program for plotting molecular and crystal structures. University of Cambridge, England, 1978.
17 J. J. P. Stewart, *J. Comput. Chem.*, 1989, **10**, 210.
18 J. J. P. Stewart, MOPAC93 Package, Revision No. 2, 1994.
19 S. P. Karna and M. Dupuis, *J. Comput. Chem.*, 1991, **12**, 487.
20 F. H. Allen, O. Kennard, D. G. Watson, L. Brammer, A. G. Orpen and R. Taylor, *J. Chem. Soc., Perkin Trans. 2*, 1987, S1.
21 J. Maurin and T. M. Krygowsky, *J. Mol. Struct.*, 1988, **172**, 413.
22 M. Krawiec and T. M. Krygowsky, *J. Mol. Struct.*, 1991, **246**, 113.
23 R. Cervellati, A. Dal Borgo and D. G. Lister, *J. Mol. Struct.*, 1981, **78**, 161.
24 E. L. Eliel, N. L. Allinger, S. J. Angyai and G. A. Morrison, *Conformational Analysis*, Wiley, New York, London, Sydney, 1965, ch. 1, pp. 6 and 22.
25 R. Glaser, G. S. Chen and C. L. Barnes, *J. Org. Chem.*, 1993, **58**, 7446.
26 M. Warner, *J. Chem. Phys.*, 1980, **73**, 5874.
27 P. A. Irvine and P. J. Flory, *J. Chem. Soc., Faraday Trans. 1*, 1984, **80**, 1821.

*Paper* 6/04300C
*Received* 19*th June* 1996
*Accepted* 6*th August* 1996